

Aggregation Kinetics of Macrocycles Detected by Magnetic Birefringence

Jeroen C. Gielen,[†] An Ver Heyen,[‡] Svetlana Klyatskaya,^{§,⊥} Willem Vanderlinden,[‡] Sigurd Höger,^{||}
J. C. Maan,[†] Steven De Feyter,^{*,‡} and Peter C. M. Christianen^{*,†}

IMM, High Field Magnet Laboratory, Radboud University Nijmegen, Toernooiveld 7, 6525 ED Nijmegen, The Netherlands, Division of Molecular and Nanomaterials and Institute of Nanoscale Physics and Chemistry, Katholieke Universiteit Leuven, Celestijnenlaan 200-F, 3001 Leuven, Belgium, Institute für Technische Chemie und Polymerchemie, Universität Karlsruhe, Engesserstrasse 16, 76128 Karlsruhe, Germany, and Kekulé-Institut für Organische Chemie und Biochemie, Rheinische Friedrich-Wilhelms-Universität Bonn, Gerhard-Domagk-Strasse 1, 53121 Bonn, Germany

Received June 12, 2009; E-mail: Steven.DeFeyter@chem.kuleuven.be; P.Christianen@science.ru.nl

Self-assembly of organic molecules offers an attractive approach for the development of potentially functional nanostructures using relatively simple molecular building blocks.¹ In contrast to the numerous investigations of the structural properties of supramolecular aggregates, only a small number of studies focus on the time scale of self-assembly,² disassembly,³ and aggregate morphology transitions.⁴ The kinetics can give valuable information on the aggregation route and the intermolecular interactions, allowing for better tuning of the molecular building blocks needed for rational design of complex functional nanostructures.^{5–7}

We have investigated the kinetics of the temperature-induced aggregation of macrocyclic molecules in solution using magnetic-field-induced birefringence. This technique is sensitive to the degree of molecular order of an entire aggregate rather than the short-range order probed by techniques such as UV–vis and circular dichroism spectroscopy. Therefore, we can distinguish ordered and disordered macrocycle aggregates in a quantitative manner. We have found that after a monomeric solution of macrocycles is cooled to a temperature T_f below the aggregation temperature, it takes days or weeks to form ordered aggregates, with a formation rate that increases with decreasing T_f . Such slow formation is unusual for individual conjugated aggregates, which exhibit typical time scales of a few seconds⁸ to several hours.⁹ We attribute this exceptionally slow behavior to the polystyrene tails of the macrocycles, which hamper the aggregation of the rigid cores.

The shape-persistent macrocycle (Figure 1a) comprises a phenylene-ethynylene-butadiynylene backbone as a rigid core.¹⁰ Four extraannular *tert*-butyl groups and two large, flexible polystyrene chains are attached to the vertices of the backbone to enhance the solubility of the molecule. The molecule possesses a large anisotropy in the diamagnetic susceptibility ($\Delta\chi \approx 10^{-7}$ m³/mol) resulting from the coplanar orientation of the phenyl rings.¹¹ An external magnetic field tends to orient such anisotropic molecules in order to minimize their magnetic energy. However, for individual molecules, the change in energy is small relative to the thermal energy. Only a large group of ordered molecules can overcome the thermal randomization and align. Therefore, only *ordered* aggregates of sufficient size can be oriented by experimentally available magnetic fields, whereas disordered aggregates cannot.¹² The induced alignment can be detected optically as magnetic-field-induced birefringence Δn (magnetic

birefringence). Since Δn depends on size, order, and aggregate density, we can follow the time-dependent aggregation process in solution in a contact-free way.

In cyclohexane, the macrocycle forms fibers that can be transferred to a mica substrate by drop-casting.^{10,11} Because of the effects of solvent evaporation and molecule–substrate interactions, atomic force microscopy (AFM) is not suited for studying the kinetics, but it is useful for visualizing the fiber morphology (Figure 1b). The fibers all have a height of 5 nm (Figure 1d) and are not clustered. The length histogram (Figure 1c) displays the typical exponential distribution expected for supramolecular aggregates¹³ (the typical length is 1.6 ± 0.1 μ m). The persistence length, important for magnetic alignment, is estimated to be 1.0 ± 0.2 μ m.¹¹

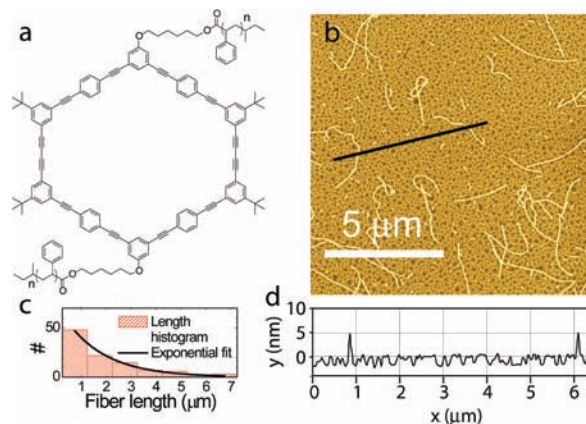


Figure 1. (a) Chemical structure of the shape-persistent coil–ring–coil macrocycle ($n \approx 25$). (b) AFM image of a 10^{-6} M solution drop-cast on mica, showing the fibers. The background layer consists of macrocycle molecules.¹¹ (c) Histogram of aggregate length (based on 103 fibers longer than 0.25 μ m, bin size = 1 μ m). The fit yields a typical length of 1.6 ± 0.1 μ m. (d) AFM cross section showing the fiber height of 5 nm.

We measured the magnetic birefringence of a 10^{-4} M macrocycle/cyclohexane solution up to 400 h after cooling to the measurement temperature T_f (10, 14, 16, or 18 °C). Between the measurements, the samples were not exposed to a magnetic field. To start, the solution was heated above 35 °C for 15 min to dissolve all of the aggregates, as verified by light scattering. The sample was then cooled to T_f using a water bath, yielding an average cooling rate of ~ 1 – 2 K/min. A T_f lower than 10 °C resulted in coagulation of the solvent ($T_{\text{melt}} = 6.59$ °C). For a T_f higher than 18 °C, no (ordered) aggregates were observed on an experimentally accessible time scale.

[†] Radboud University Nijmegen.

[‡] Katholieke Universiteit Leuven.

[§] Universität Karlsruhe.

^{||} Universität Bonn.

[⊥] Present address: Forschungszentrum Karlsruhe GmbH, Institut für Nanotechnologie, Hermann-von-Helmholtz-Platz 1, 76344 Eggenstein-Leopoldshafen, Germany.

A typical magnetic birefringence curve is shown in the inset of Figure 2a and resembles the usual S-shaped curve.¹² For low field strengths, Δn increases quadratically with B , followed by a slower increase in the intermediate regime up to 20 T. Application of higher fields would further increase the alignment until the birefringence saturates, but this would require fields higher than 20 T for the macrocycle aggregates.

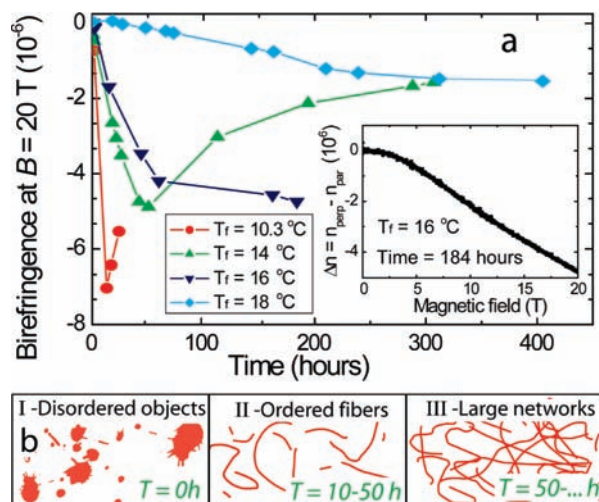


Figure 2. (a) Solution birefringence at $B = 20$ T as a function of time for different temperatures T_f . The inset shows a full birefringence curve. (b) Schematic representation of the situation at $T_f = 14$ °C, showing the transition from disordered objects (I) to ordered fibers (II) to a large network of fibers (for low T_f) (III).

Figure 2a shows the magnetic birefringence caused by the macrocycle alignment at $B = 20$ T as a function of time after cooling. We can distinguish three different time regimes, which we will discuss on the basis of the $T_f = 14$ °C measurements. Immediately after the system is cooled, there is no birefringence signal, and there is no shift in the UV-vis absorbance spectrum that would indicate aggregation.¹¹ However, light scattering experiments indicated the presence of large objects characterized by strong scattering, predominantly at small scattering vectors.¹¹ The absence of both a magnetic birefringence signal and a shift of the absorbance maximum proves that these objects have a negligible degree of (long-range) order (regime I in Figure 2b).

During a period of a few days, the disordered objects are transformed into ordered fibers, which can be aligned in a magnetic field (regime II), causing Δn and the aggregate absorbance to increase in time. We can exclude the presence of other aggregate morphologies, since AFM¹¹ and small-angle X-ray scattering¹⁴ have shown that over a range of concentrations and temperatures, only fiber-shaped aggregates exist in equilibrated solutions. From fitting the shapes of the Δn curves, we found that on average an aggregate consists of 5000 molecules.¹¹ If an intermolecular distance of 0.6 nm is assumed,¹⁴ this corresponds to an average fiber length of 2–3 μm , which agrees reasonably well with the length found by AFM for $C = 10^{-6}$ M.

After 50 h, the fibers slowly cluster to form a network (regime III), causing a reduced Δn . We verified that this reduction was not caused by precipitation.¹¹ The network formation only occurs for $T_f < 16$ °C and can be observed with the naked eye.¹¹ A small rise in temperature quickly breaks up this network; drop-casting a solution with networks on mica at room temperature still results in individual fibers on the substrate (Figure 1b).

The time scale on which these changes take place is slow and strongly temperature-dependent: the lower T_f , the faster the kinetics. At $T_f = 18$ °C, the transformation of disordered objects to ordered fibers takes more than 300 h, whereas this time shortens to 50 h at 14 °C and to 10 h at 10 °C. These time scales were confirmed by UV-vis absorbance measurements.¹¹ Only for $T_f = 18$ °C was the fraction of aggregated material too low to observe a change in the absorbance spectrum upon aggregation. This further confirms the usefulness of magnetic birefringence as compared with UV-vis absorbance.

We speculate that the kinetics is influenced by the long, flexible polystyrene tails, which have temperature-dependent solubility and extension; the presence of the tails can hinder the ordered stacking of monomer cores. As a result, cooling a monomeric solution leads to the fast formation of large disordered objects that are slowly converted into thermodynamically stable, ordered fibers, either directly or via an intermediate step of monomers. The conversion kinetics depends on the energetic landscape, including the barriers between the monomeric-, ordered- and disordered states, each of which can depend on temperature in a different way, causing the unexpected inverse temperature dependence of the fiber formation rate.

In conclusion, we have used magnetic birefringence as a new, sensitive technique to probe the kinetics of molecular aggregation. We have found three consecutive stages for the macrocycle system: disordered objects, ordered fibers, and a network. The transition rate from disordered objects to ordered conjugated fibers is low and increases with decreasing temperature T_f . Linking aggregation kinetics to molecular properties will lead to a better understanding of the mechanisms by which molecules self-assemble, allowing for a more rational design of the organic molecular building blocks.

Acknowledgment. Part of this work was supported by Euro-MagNET (RII3-CT-2004-506239), KU Leuven (GOA 2006/2), the I.W.T., the FWO, the Belgian Federal Science Policy Office (IAP-6/27), and the DFG. We thank A. J. M. Giesbers for additional AFM images.

Supporting Information Available: Detailed procedures and light scattering, AFM, UV-vis, and birefringence data. This material is available free of charge via the Internet at <http://pubs.acs.org>.

References

- (1) Service, R. F. *Science* **2005**, *309*, 95.
- (2) (a) Pasternack, R. F.; Gibbs, E. J.; Collings, P. J.; dePaula, J. C.; Turzo, L. C.; Terracina, A. J. *Am. Chem. Soc.* **1998**, *120*, 5873. (b) Kersemakers, J. W. J.; Munteanu, E. L.; Laan, L.; Noetzel, T. L.; Janson, M. E.; Dogterom, M. *Nature* **2006**, *442*, 709.
- (3) Pasternack, R. F.; Gibbs, E. J.; Bruzewicz, D.; Stewart, D.; Engstrom, K. S. *J. Am. Chem. Soc.* **2002**, *124*, 3533.
- (4) Zhang, L.; Eisenberg, A. *Macromolecules* **1999**, *32*, 2239.
- (5) Jyothish, K.; Hariharan, M.; Ramaiah, D. *Chem.—Eur. J.* **2007**, *13*, 5944.
- (6) Pasternack, R. F.; Fleming, C.; Herring, S.; Collings, P. J.; dePaula, J.; DeCastro, G.; Gibbs, E. J. *Biophys. J.* **2000**, *79*, 550.
- (7) Lohr, A.; Lysetska, M.; Würthner, F. *Angew. Chem., Int. Ed.* **2005**, *44*, 5071.
- (8) Smulders, M. M. J.; Schenning, A. P. H. J.; Meijer, E. W. *J. Am. Chem. Soc.* **2008**, *130*, 606.
- (9) Pasternack, R. F.; Gibbs, E. J.; Sibley, S.; Woodard, L.; Hutchinson, P.; Genereux, J.; Kristian, K. *Biophys. J.* **2006**, *90*, 1033.
- (10) (a) Rosselli, S.; Ramminger, A. D.; Wagner, T.; Silier, B.; Wiegand, S.; Haussler, W.; Lieser, G.; Scheumann, V.; Hoger, S. *Angew. Chem., Int. Ed.* **2001**, *40*, 3138. (b) Rosselli, S.; Ramminger, A. D.; Wagner, T.; Lieser, G.; Höger, S. *Chem.—Eur. J.* **2003**, *9*, 3481.
- (11) See the Supporting Information.
- (12) Christianen, P. C. M.; Shklyarevskiy, I. O.; Boamfa, M. I.; Maan, J. C. *Phys. B* **2004**, *346–347*, 255.
- (13) Van der Schoot, P. In *Supramolecular Polymers*, 2nd ed.; Ciferri, A., Ed.; CRC Press: Boca Raton, FL, 2005.
- (14) Dingenouts, N.; Klyatskaya, S.; Rosenfeldt, S.; Ballauff, M.; Höger, S. *Macromolecules* **2009**, *42*, 5900.

JA904816M